J Inorg Organomet Polym (2017) 27 (Suppl 1):S189–S200
DOI 10.1007/s10904-017-0665-y

Investigation in Mediated Heterogeneous Oxygen Reduction of Immobilized Laccase

Yu He Zhang[1] · Yang Yang[1] · Han Zeng[1] · Wen Shan Huo[1]

Received: 6 June 2017 / Accepted: 28 August 2017 / Published online: 2 September 2017

Abstract Dynamics of heterogeneous catalysis on oxygen reduction for Lac based electrode capped with a layer of Chitosan-multi-wall carbon nano-tubes complex in the presence of dissolved mediator, was investigated on the basis of precondition that the detainment of substrate and mediator could be neglected. Rates of steps involved in the whole catalytic cycle were determined by the means of UV–Vis spectroscopy, atomic adsorption spectroscopy, linear sweeping voltammetry and cyclic voltammetry in combination with rotating disk electrode technique. These kinetic parameters were normalized under the same dimension. Thus rate determining step was verified to be the diffusion of external mediator. Results also revealed the fact from analysis in changes of morphology and electric conductivity after protein incorporation into nano-composite that random adsorption of enzyme molecules on the conductive support resulted in the decrease in conductive area of nano-composite and hindered the direct electron transfer between active sites in enzyme molecules and conductive matrix. Non-oriented arrangement of protein molecules on the matrix also crippled the mechanical stability of nano-complex with enzyme resulting from weak interaction between incorporated protein molecules and carrier.

✉ Han Zeng
zenghan1289@163.com

[1] Key Laboratory of New energy and Novel Materials, Chemistry and Chemical Engineering Academy, XinJiang Normal University, Ürümqi 830054, People's Republic of China

Graphical Abstract Catalytic effect on dissolved oxygen reduction reaction for electrode which was over-coated by a layer of nano-complex with immobilized Laccase consisting of Chitosan and multi wall carbon nano-tubes, were found to be restrained by diffusion of electron relay.

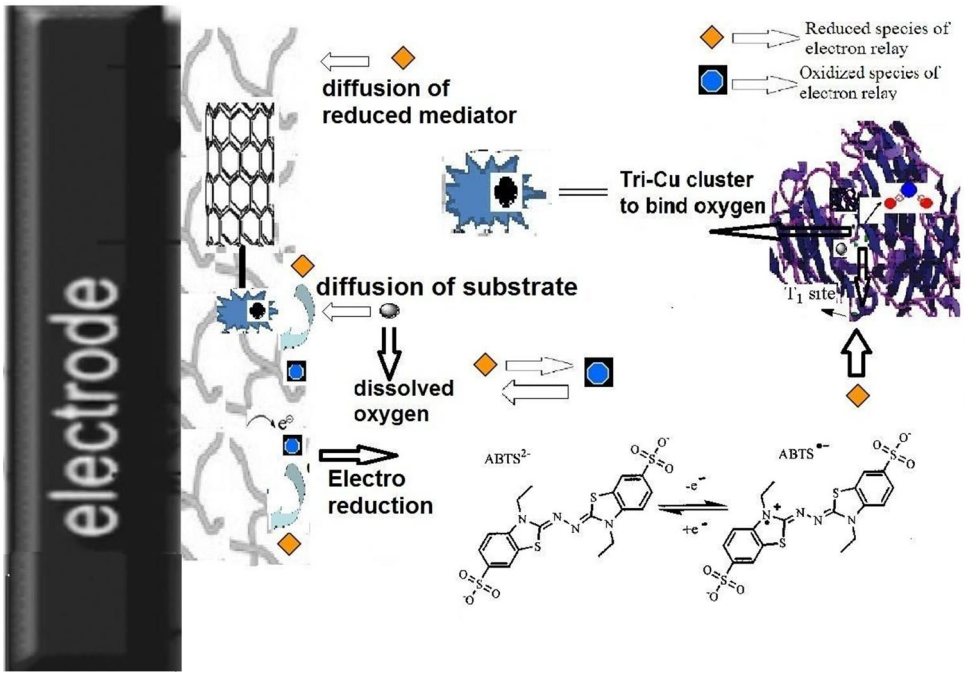

Keywords Carbon nano-tubes · Chitosan · Heterogeneous catalysis · Mediator · Rate limiting step

1 Introduction

Enzymatic fuel cells have been investigated extensively for decades. Aim of research for scientific society and industrial interest is to seek out the optimal proto-type with high performance in energy out-put. This favorable enzyme based fuel cell has some advantages such as its friendliness to environment and organism, low-cost and renewability [1, 2]. Improvement in the dynamics of enzyme induced catalysis is considered to be the foremost step proverbially in modeling the desirable enzymatic fuel cell. Although the mode of direct electron transfer is regarded as the most efficient approach to achieve this goal, sophisticated structure of redox protein and complicated interactions between enzyme carriers and entrapped protein molecules render these attempts impossible to some extents [3–6]. Thus the mode of mediated electron shuttle between enzyme and conductive support in the aid of external electron relay still remains to be the most feasible means [7, 8].

Early cases of catalytic reactions for enzymatic fuel cells with the mode of mediated electron transfer should be ascribed to be a typical class of homogeneous catalysis. Such shortcomings as failure to recovery of biocatalyst, expensive cost of operation and inferior long-term stability would cripple its wide application in practice substantially [9, 10]. Later another mediated enzymatic cell on the basis of heterogeneous catalysis is proposed to fix these issues, meaning either redox proteins or electron mediator molecules are integrated into matrix [11–13]. It should be noted that enzyme induced catalysis with the help of external electron mediator still remains inferior long-term stability of catalytic performance and potential harm to orgamism and environment [14, 15].

Models concerning about the dependence of catalytic current density for enzyme based electrode on rate of over-all reaction for enzymatic catalysis, have been proposed for decades [16, 17]. It should be noticed that derived conclusions could only be applied to the case of homogeneous catalysis. Some discussions in recent years [18, 19] have been made on the aspect of kinetics in heterogeneous catalysis where redox protein molecules are immobilized in specific matrix. Conclusions from these investigations only provide over-all rate of catalysis and they fail to make specific analysis to each step involved in the catalysis. More importantly rate determining step in the whole catalysis hasn't been designated for most systems yet [16–19]. This article focused on a typical case of heterogeneous enzymatic catalysis which

bases on nano-composite with accommodated protein molecules which was made up of carbon nano-tubes and polymer in the presence of electron relay dissolved in electrolyte. It should be stressed that efficient catalysis to oxygen reduction reaction (ORR) for this system has been achieved and relevant analysis has been demonstrated by Dong and her co-workers [20]. However contribution of each procedure to the whole catalytic cycle hasn't been verified yet. This paper made systematic evaluation in enzyme induced heterogeneous catalysis and divides the whole catalysis into three segments to secure rate constants by the means of electrochemistry and spectrometry. Rate limiting step could be affirmed through comparison in rate constants of steps for the enzymatic catalysis under the same dimension. Validity of conclusions in this submission was evaluated after the application of them to other similar systems.

2 Experiment

2.1 Reagents and Apparatus

Laccase (abbr. Lac from *Trametes versicolor* was purified according to the same procedure which was introduced by Zheng [21]). 2,2′-azino-bis-(3-ethylbenzothiazoline-6-sulphonic acid) diammonium salt (ABTS) and 2,6-dimethoxyphenol (DMP) were purchased from Sigma-Aldrich chemical reagent Co., Ltd. Chitosan (CTS, M_w: 2.5×10^5, deacetylation level $\geq 90\%$) was obtained from Shanghai Shengyao Biotech Co, Ltd (China). Multiwall carbon nanotubes (MWCNTs, from Shenzhen Nanotech. Port. Co, Ltd, Shenzhen, China) was pretreated as the description which has been published elsewhere [20]. Other commonly used chemicals from Sinopharm Co., Ltd in China were of analytical level. Electrolyte solution in this manuscript was 0.2 M phosphate buffer (abbreviated as PBS). pH of buffer solution was manipulated through the adjustment in scale of K_2HPO_4 and citric acid amount. Milli-Q ultrapure water (from Millipore Q water treatment apparatus with resistivity up to 18 MΩ cm) was used throughout. Gases (N_2 and O_2) which were bubbled into the electrolyte solution, were available commercially from NanJing special gas Co., Ltd in China. TG16WS type high speed centrifuge (Xiangyi Co., Ltd, in China) was adopted to separate MWCNTs from supernatant of rinse solution. Morphology of nano-complex with Lac was characterized with AMT XR401 transmission electron microscope (available from Advanced Microscopy Techniques Company, in USA, operation at accelerating voltage of 100 kV). Change in electric conductivity of nano-complex before and after enzyme immobilization was determined with Zahner Zennium electrochemical analyzer (Kronach, in Germany) and data were recorded in electrolyte with 5.0 mM $K_3Fe(CN)_6 + 0.1$ M KCl. Tests of impedance were operated under the amplitude of inspired signal at 5 mV and frequency range of $0.5–10^5$ Hz.

2.2 Determination in Dynamics of Lac Induced Chemical Reaction and Mass Transferring

Preparation of Chitosan-MWCNTs nano-composite with entrapped Lac molecules was illustrated previously [20]. Mass transferring segment included diffusion processes of electron relay and substrate between bulk solution and the surface of electrode over-coated by layer of nano-complex with Lac. Rate of mass delivering for substrate: di-oxygen in electrolyte was estimated with the help of the Fick's 2nd diffusion law. Rate for diffusion of electron mediator (reduced and oxidized species) in PBS was measured by electrochemical means [i.e. cyclic voltammetry (CV) or linear sweeping voltammetry (LSV)]. It indicated this parameter could be calculated from the slope of calibrated curve which represented the dependence of redox peak current on square root of scanning rate. This parameter could also be derived from the slope of plot which reflected the relationship between limited current density and square root of rotating rate for disk electrode. Related equations and their premises of applications have been described elsewhere [22, 23]. PBS with primitive ABTS was purged with N_2 for 30 min at least to expel oxygen from electrolyte entirely and N_2 atmosphere was retained in the procedure of determination in the diffusion coefficient for reduced state of ABTS. PBS with co-dissolved Lac and original ABTS was bubbled with oxygen for at least 1 h to secure oxygen-saturated electrolyte with fully oxidized ABTS and O_2 atmosphere was kept during the measurement in the diffusion coefficient for oxidized species ofABTS. Specific immobilization mass of Lac (i.e. normalization of mass for incorporated redox protein to that of carrier) was determined by graphite furnace atomic adsorption spectrometer (Hitachi z2000 type with wave length ranging from 190 to 900 nm, from Hitachi Co., Ltd. in Japan). It indicated this parameter could be calculated from the change in consistency level of Cu in bulk solution before and after Lac integration into the matrix which was described previously [24]. Rate for enzymatic oxidation of reduced ABTS was measured with UV–Vis spectroscopy (optical path: 1 cm, U-2810 spectrophotometer from Shimadzu Company, Japan) at the wavelength of maximum absorbance for oxidized mediator. Normalized rate constant for this enzymatic reaction could be derived from the definition of specific activity of enzyme induced catalysis [10, 25]. Furthermore binding rate of oxygen on cofactors of Lac entrapped in matrix could be figured out with the change in consistency levels of dissolved substrate which were determined by Clark type oxygen electrode available from Hansatech Company of UK. This parameter can also

be estimated roughly with chronoamperometry only when the rate of oxygen attachment was faster than that of the electrochemical reduction of oxidized mediator.

2.3 Determination in Kinetics of Mediated Electron Transfer for Nano-Composite Based Electrode with Lac

Dynamics of mediated electron shuttle was probed by LSV with the help of rotating disk electrodes technique (AFM-SRCE rotating disk electrode system was available from Pine Company, USA. Rotating speed of electrode ranged from 50 to 10,000 round/min). A typical 3-electrodes cell was proposed in tests. Basal glassy carbon electrode (abbr. GCE with diameter of 4 mm from Tianjin Aida Hengsheng Co., Ltd. China) over-coated by a layer of nano-composite with Lac was proposed to be working electrode. Potentials of electrode in this article were values relative to reference electrode: Ag/AgCl (saturated KCl solution). Do-it-yourself platinum spire served as auxiliary electrode. All electrochemical experiments were conducted on CHI-1140A electro-chemical station (Shanghai Chen-Hua Instrument Co., Ltd. China) which was connected to a typical commercial computer. Standard rate for electro-reduction of oxidized mediator could be derived from normalization of rate determined with electrochemical means (dimension: cm/s) to thickness of reaction layer which was definite previously [18]. CV curves in this manuscript were recorded in the steady status (i.e. CVs should be over-lapped at different rounds).

2.4 Mechanical, Thermal Stability and Acid-Base Endurance of Nano-Composite Based Electrode

In order to evaluate the mechanical stability of enzyme based electrode against shear stress resulting from the rotating of electrode, disk electrode was immersed into oxygen bubbled electrolyte in the absence of electron relay and the experiments were performed under variable rotating rates. Disk electrode was separated from the buffer solution after incubation for 10 min and oxygen-purged PBS containing 10.0 mM DMP was then injected into the latter. Changes in absorbance at 470 nm for buffer solution with time lapse were recorded subsequently.

Thermal stability and acid-base endurance of Lac-based electrode were investigated through monitoring the variation in limited catalytic current with alterative pH value of electrolyte and operating temperature at constant applied potential, repectively. It should be noted these measurements were performed under static status.

3 Results and Discussion

3.1 Kinetics of ABTS Mediated Oxygen Reduction Reaction for Lac-Induced Catalysis

3.1.1 General Analysis in Lac Induced Catalysis to Oxygen Reduction Reaction

Analysis to changes in morphology and electrical conductivity of nano-composite before and after Lac integration were made on the basis of tests for microscopy and impedance. Results from experiments indicated that amorphous cluster resulting from non-orientated adsorption of Lac onto the surface of nano-composite and apparent increase in charge transferring resistance were observed in transmission electron microscopy (TEM) images (Fig. 1) and electrochemical impedance spectra (EIS) (Fig. 2). They provided side proofs to support the conclusion that direct electron transfer between enzyme and conductive matrix failed to achieve for Lac immobilization in nano-complex. Actually the essence of mediated catalysis to ORR for Lac based electrode should be ascribed to a typical so-called ping pong mechanism which comprised of Lac induced chemical oxidation of mediator and concurrent transformation of binding di-oxygen molecules into H_2O molecules together with simultaneous electro-chemical reduction of oxidized species of mediator (ABTS) (i.e. regeneration of mediator). Case of heterogeneous catalysis was distinct from that of homogeneous catalytic reaction where enzyme and electron mediator co-dissolved in electrolyte. Kinetics of former was more complicated than that of latter in that several sub-divisions [14, 26]. They included co-immobilization of enzyme and mediator into carrier in the absence of substrate retention within supporting matrix (this precondition was supported by the fact that MWCNTs didn't exhibit its competency to accommodate di-oxygen molecule and drop in oxygen consistency level of electrolyte wasn't detected

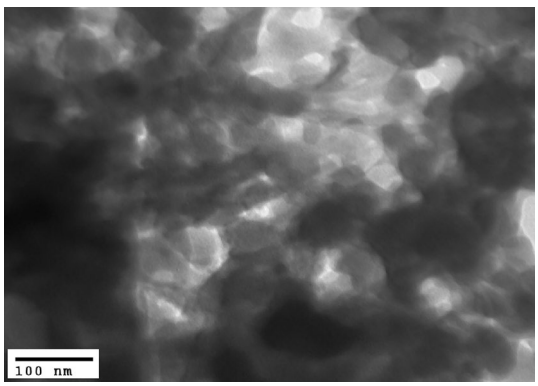

Fig. 1 TEM image of CTS-MWCNTs nano-composite with integrated Lac

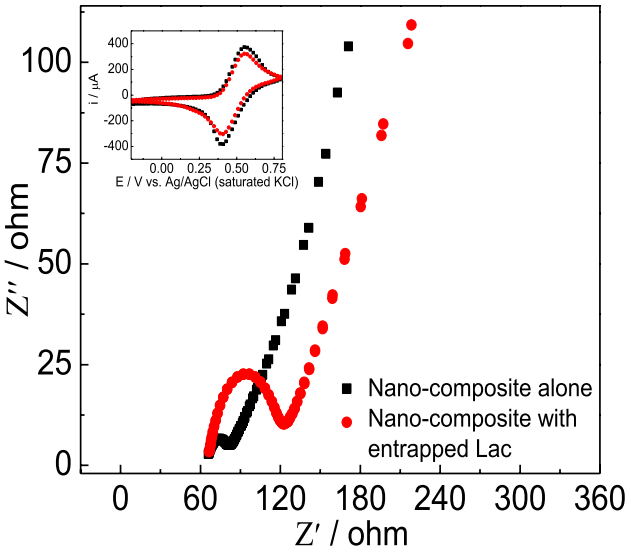

Fig. 2 EIS spectra of CTS-MWCNTs nano-composite itself modified electrode and electrode over-coated by a layer of nano-complex with incorporated enzyme molecules, *inset graph* cyclic voltammograms of both electrodes recorded at scanning rate of 100 mV/s. Supporting electrolyte: aqueous solution containing 5 mM $K_3Fe(CN)_6$ + 0.1 M KCl

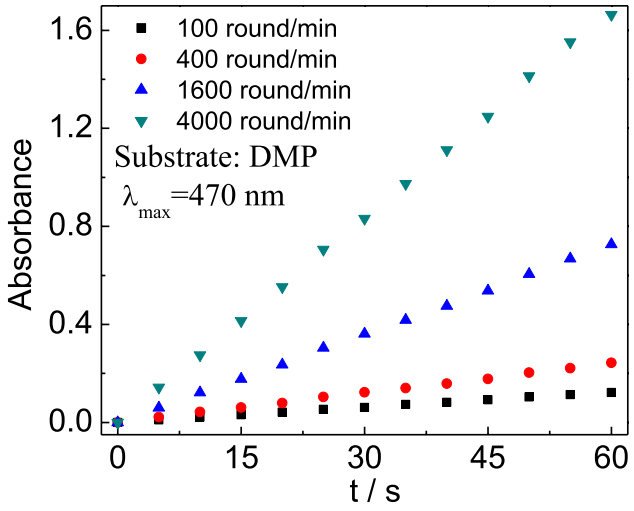

Fig. 3 Leaching test for nano-composite with Lac characterized by UV–Vis spectroscopy when disk electrode operated under variable electrode rotating rates and in oxygen bubbled PBS (pH 4.4)

with Clark oxygen electrode after adequate incubation of MWCNTs based electrode with air-saturated solution.), and protein incorporation alone in matrix with partial detainment of substrate: di-oxygen molecules and/or electron mediator in nano-composite in the presence of external electron relay dissolved in buffer solution. Former case indicated that mode of charge shuttle was distinguished from that of homogeneous catalysis in so-called "hopping mode of electron transfer between immobilized electron relay and conductive interface and homogeneous chemical reaction between electron mediator and redox enzyme similar to homogeneous catalysis induced by protein. Latter one was more sophisticated in hybrid of heterogeneous and homogeneous electrochemical reaction and/or enzymatic chemical reaction which occurred within the matrix on the interface of electrode and/or on the surface of thin film with integrated protein molecules. It meant the elevated difficulty in analysis to steps of the whole catalytic cycle. Both cases were beyond the reach of investigation in this manuscript. In another word, the case that the retention of substrate and mediator in nano-complex with integrated Lac could be negligible, was considered to be the simplest one in all sub-divisions of heterogeneous catalysis for Lac-based electrode (this premise can be met for this sub-case in this article and supporting proofs can be found in the following Sect. 3.1.4). It should be noted that the mechanical stability of as-prepared Lac-based electrode was not desirable. This conclusion was supported by the fact from analysis in Fig. 3 that absorbance of solution at wavelength of maximal absorption increased rapidly when the rotating rate of disk electrode was higher than 400 round/min. It indicated that the apparent leakage of enzyme from the carrier to the electrolyte can be confirmed through this test. Enzyme induced catalytic ORR for this Lac-based electrode should be divided into several steps as illustration in Fig. 4: (1) mass transferring of mediator and substrate; (2) electro-reduction for oxidized species of electron mediator which was generated by Lac immobilization in nano-composite; (3) Chemical reactions composing of Lac-induced oxidation for reduced form of ABTS, substrate binding and transformation on active sites of redox protein molecules in incorporated status. Rate constants for those steps were compared under the same dimension through proper normalization and rate limiting step could be affirmed accordingly.

3.1.2 Dynamics in Mass Transferring of Substrate and Mediator

Rate constants of diffusion for substrate and mediator (i.e. dimension: s^{-1}) were derived from normalization of coefficients in mass transferring (dimension: cm^2/s) for them to area occupied by protein (dimension: cm^2), respectively. Rate in mass transferring for substrate: di-oxygen within the electrolyte was estimated to be 1.7×10^{-5} cm^2/s which was illustrated elsewhere [22]. Existence of ABTS in the PBS purged with N_2 or electrolyte saturated with air for a short period should be dominated by reduced state in the absence of Lac. Thus diffusion constant for reduced ABTS was estimated to be 5.0×10^{-6} cm^2/s from mean value of slopes in relationship curves of oxidation and reduction peak currents vs. square root of scanning rates which originated from CV curves of nano-complex based electrode with Lac as demonstration in Fig. 5a and its inset graph, respectively. Reduced

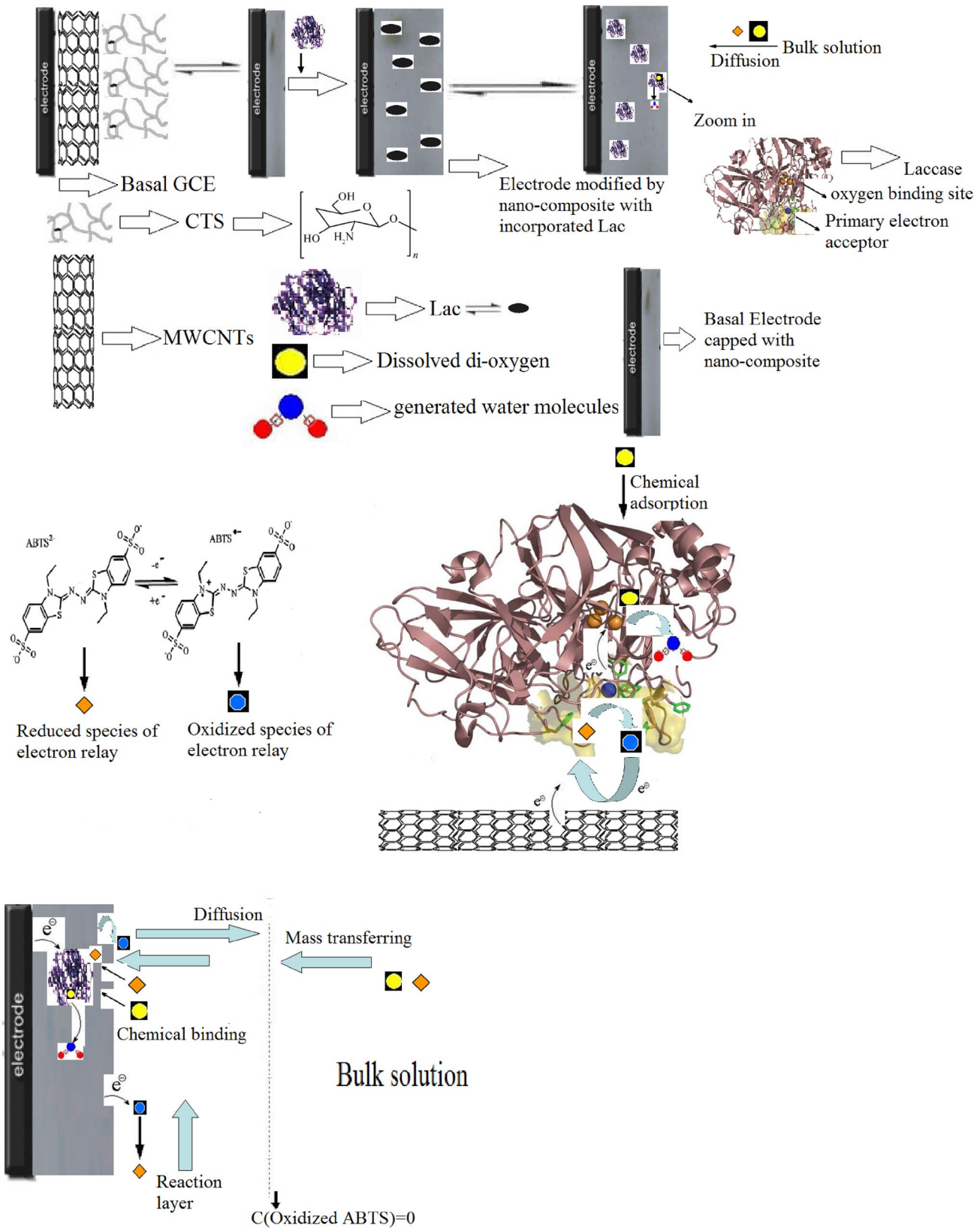

Fig. 4 Schematic illustration of heterogeneous catalysis to oxygen reduction reaction in respect to enzyme incorporation and without detainment of mediator and substrate into matrix

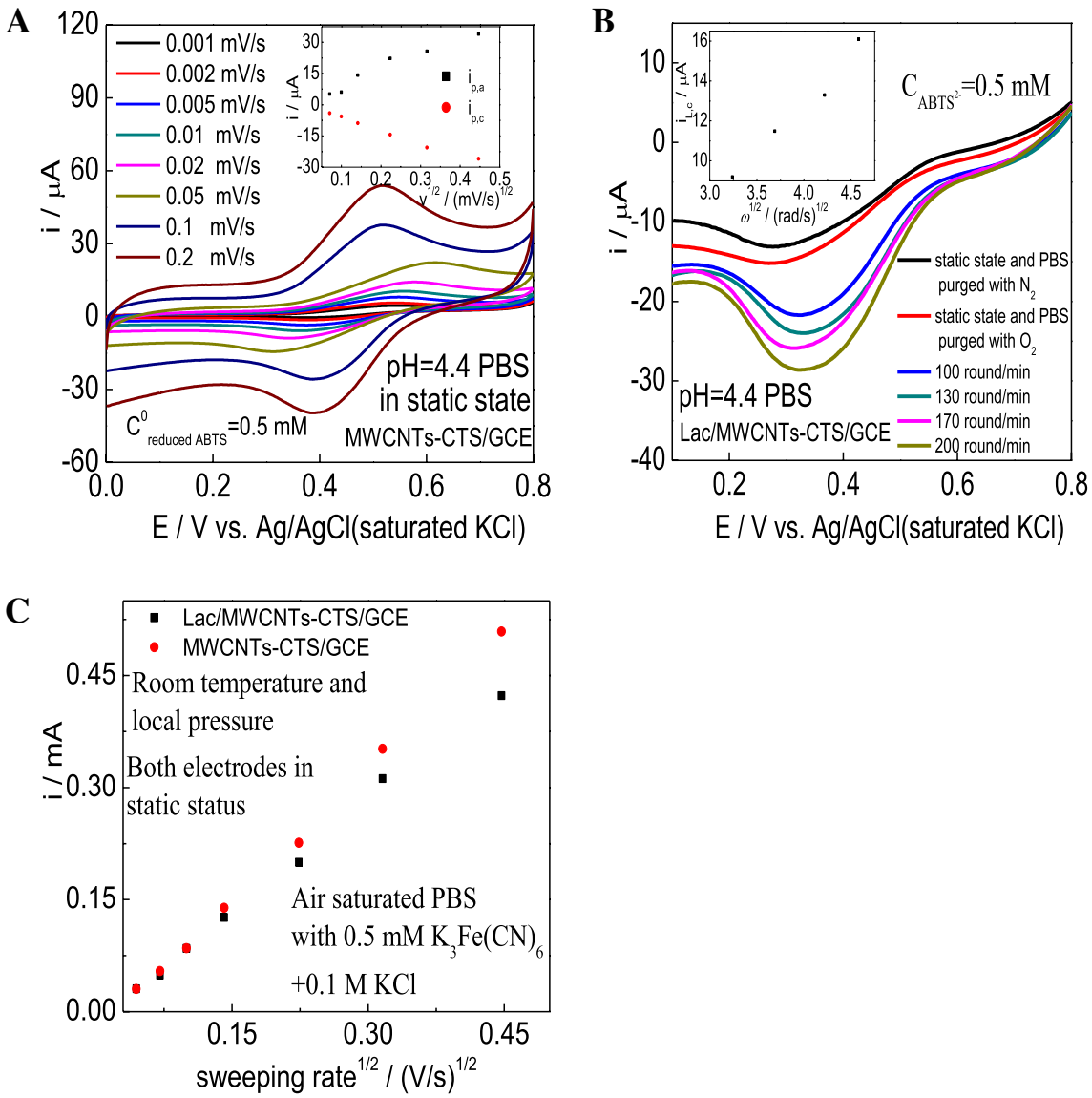

Fig. 5 Cyclic voltammograms of nano-complex based electrode without Lac in PBS containing 0.5 mM ABTS recorded under dissimilar sweeping rates when electrode in static status (**a**) and its *inset graph* dependence plots of anodic and cathodic peak current on square root of scanning rate, respectively; Linear sweeping voltammograms of GCE over-coated by nano-composite with incorporated Lac in oxygen-saturated PBS with 0.5 mM $ABTS^{2-}$ which were recorded under variable rotating rates and at scanning rate of 30 mV/s (**b**), its *inset graph* calibration *curve* of cathodic limit diffusion current against square root of rotating rate; Dependence plots of average value for reduction and oxidation peak currents against square root of potential scanning rates for both electrodes: nano-composite based GCE and GCE over-coated by nano-complex after Lac incorporation in PBS containing 0.5 mM $K_3Fe(CN)_6$ and 0.1 M KCl (**c**)

state of ABTS was incubated adequately with primitive Lac in the presence of O_2 and then fully transformed into oxidized species. Diffusion coefficient of oxidized ABTS was measured with LSV in combination with rotating disk electrode technique. In briefly, limiting diffusion currents in *i–E* curves for Lac-based electrode immersed into oxygen-bubbled PBS with ABTS at constant consistency and under controllable rotating rates, were plotted against square roots of angular velocities of disk electrode. Relevant results were exhibited in Fig. 5b and its inset graph. Thus this parameter was calculated to be 5.0×10^{-6} cm^2/s according to the slope from inset graph of Fig. 5b. Protein coverage area was calculated through deduction of conductive area after Lac integration into nano-composite from total area of nano-composite which allowed electron shuttle. Feasibility of this approach was supported by the fact which was provided previously (i.e. EIS spectra in Sect. 3.1.1) and it can be applied to other similar systems which has been depicted previously [6]. Both of them were determined to be 0.26 and 0.32 cm^2 from CVs for Lac-based electrode and nano-composite alone

modified electrode in PBS containing 0.5 mM $K_3Fe(CN)_6$ and 0.1 M KCl which were recorded under variable sweeping rates as demonstration in Fig. 5c. Relevant method and equations were displayed elsewhere [27]. Thus rate constants of mass transferring for oxygen, reduced ABTS and oxidized mediator were normalized to be 3.2×10^{-4}, 9.4×10^{-5} and 9.4×10^{-5} s^{-1}, respectively. Surface coverage of enzyme molecules was deduced to be 2.5×10^{-13} mol from normalization of difference in proportions between both electrodes to footprint (35.8 nm^2, this value has been illustrated previously [25]) of Lac.

3.1.3 Dynamics of Enzyme Induced Chemical Reactions

Figure 6a displayed the relationship curve for absorbance of electrolyte which was osculated sufficiently with Lac entrapment in nano-complex against time lapse. It can be seen from Fig. 6a linear response between absorbance of supernatant (A) and testing time can be maintained within testing time window. Rate of Lac-induced catalysis to oxidation of $ABTS^{2-}$ (R_{ox}) could be determined to be 1.6×10^{-9} mol/s from slope of linear fitting plot in Fig. 6a and equation: $A=\varepsilon bc$ (b is optical length: 1 cm, ε means the molar

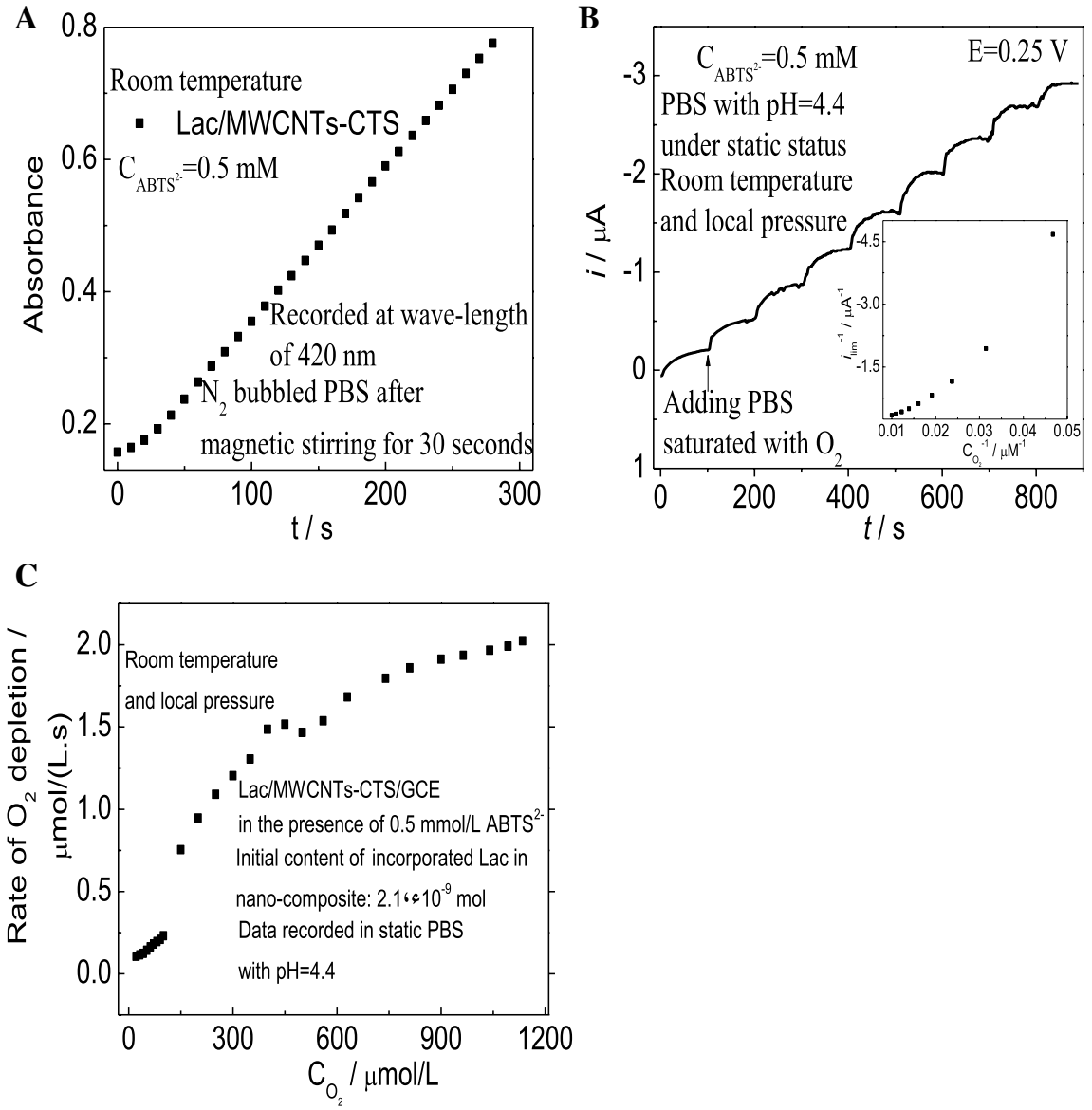

Fig. 6 Dependence plot of absorbance for PBS containing ABTS which had been contacted adequately with nano-complex with incorporated Lac on testing time (**a**); chronoamperometric *curve* of nanocomposite with Lac modified GCE in static PBS with variable consistency levels of O_2 and 0.5 mM ABTS which was recorded under applied potential of 0.25 V (**b**), its *inset graph* was double reciprocal curve of limiting reduction current against substrate consistency for Lac/MWCNTs-CTS/GCE; Dependence of O_2 depletion rate on content of di-oxygen in static PBS with pH 4.4 and 0.5 mM ABTS for nano-composite based electrode with Lac (**c**)

extinction coefficient for free radical of ABTS at 420 nm which was illustrated elsewhere [28]: 3.6×10^{4} M^{-1} cm^{-1} and c is bulk concentration of ABTS). Furthermore enzyme loading amounts in nano-composite was measured to be 2.1×10^{-9} mol according to the method introduced in Sect. 2.2 (i.e. specific accommodation amount of Lac into matrix was 48.0 mg/g). Therefore normalized rate constant of enzymatic oxidation (k_{ox}) of reduced ABTS was derived to be 7.6×10^{-1} s^{-1} in the light of the formula: $R_{ox}=k_{ox}\times n_E$ (n_E was designated to be the immobilized amount of Lac within nano-complex). Figure 6b and its inset graph displayed the typical curve of steady-state current *vs*. working time and double reciprocal calibration plot of limiting diffusion current against substrate consistency for nano-complex modified electrode with Lac working in static PBS containing 0.5 mM ABTS and at applied potential of 0.25 V, respectively. Depletion rate of dissolved oxygen could be estimated through normalization of change in oxygen contents to the time intervals between adjacent steady current steps in Fig. 6b. It should be noted the measured result was in accordance with that monitored withClark oxygen electrode. Michaelis–Menten constant of nano-composite based electrode with Lac to substrate: O_2 (K_s) was calculated to be 0.353 mM from inset graph of Fig. 6b. Rate constant for oxygen binding on active site of Lac was deduced to be 492.0 s^{-1}. This value originated from plot of consumption rate for di-oxygen dissolved in PBS versus initial concentration of oxygen in electrolyte as demonstration in Fig. 6c and could be derived according to specific description and related equations described previously [16]. This value was consonant with the deduced one of enzymatic catalysis in the light of the equations which reflected the dependence of limited steady current (data from repetition of tests which were demonstrated elsewhere [20]) on rate of overall catalytic reaction (k_{cat}) and apparent rate constant of enzymatic catalysis. Rate constant in transformation from attached di-oxygen on binding pocket of Lac into water molecules couldn't be measured directly under the current condition. It should be noticed that the apparently enhanced current of electro-reduction for oxidized ABTS in oxygen-saturated PBS was observed in the presence of immobilized Lac after comparison with that of the same electrode in oxygen-free electrolyte which has been displayed previously [20, 23]. It suggested that the rate in conversion of binding substrate into product should be the same magnitude as that in electro-reduction of oxidized electron relay.

3.1.4 Kinetics of Electrochemical Reduction for Electro-Active Species

Rates of electro-reduction for oxidized ABTS (k_) at different over-potentials (η) could be estimated through the equation: $i_k=nFAk\_C_{ABTS}$ which was depicted elsewhere [23]. Here i_k meant utterly dominating current of kinetics which was reciprocal of the extrapolated intercept from the plot of 1/i versus $\omega^{-1/2}$ (ω was rotating angular rate of disk electrode) at an infinitely high rotating rate. Thus standard rate at formal potential of electro-active species (k_0, dimension: cm/s) would be calculated from Fig. 7a and its inset graph with the help of equation $k\_=k_0\exp(\beta nF\eta/RT)$, β was denoted to be the co-efficient of charge shuttle and was calculated roughly to be 0.84.

Thickness of reaction layer (μ) was calculated in term of Eq. (3.1) which was deduced after moderate modification to its original form which was illustrated elsewhere [18]. Thus μ was estimated to be 8.8×10^{-3} cm. This parameter originated from the diffusion law of Fick: $V_E\times\mu=D_M(d[M_{OX}]/dx)_{x=0}$. V_E was apparent rate of enzymatic reactions with bi-ping pang mechanism which was formulated previously [16, 18], $[M_{OX}]$ meant the content of oxidized mediator, D_M was designated to be the coefficient of diffusion for electron relay and x was the distance from the surface of the electrode modified by nano-complex with protein to somewhere in bulk solution. $n_{0,ABTS}$ indicated initial concentration of mediator in electrolyte and C_{oxygen} meant total concentration of dissolved di-oxygen in buffer solution.

$$\mu=[D_M n_{0,ABTS}(C_{oxygen}+K_S)/k_{cat}n_E C_{oxygen}]^{1/2} \tag{3.1}$$

in the case of $K_M<<[M_{OX}]$ which was presented elsewhere [20].

Thus the normalized rate constant for electro-chemical reduction of oxidized ABTS was estimated to be 1.1×10^{-3} s^{-1} through normalization of k_0 to μ. This value was much lower than that (0.19 s^{-1}) described elsewhere [23]. It could be ascribed to the existence of non-conductive protein molecules and electro-static attraction to oxidized ABTS for immobilized Lac in the weak acidic buffer solution which prevented electro-active species approaching the surface of conductive support to undergo electrochemical reduction for its regeneration. It should be noted that all these conclusions were based on premise which had been demonstrated previously. It indicated that neglect for detainment of electron mediator and substrate in nano-composite can be considered to be reasonable. This premise could be met according to the analysis to results which were displayed in Fig. 7b, c (Result from Fig. 7b showed that reduction current decreased rapidly and then attained a plateau region with time lapse for electrode capped by nano-composite with Lac which was contacted adequately with oxygen purged PBS firstly and was immersed into nitrogen bubbled PBS containing ABTS subsequently (i.e. if nano-composite had competency to accommodate oxygen, reduction current could be detected whether the presence or the absence of the electron mediator). This

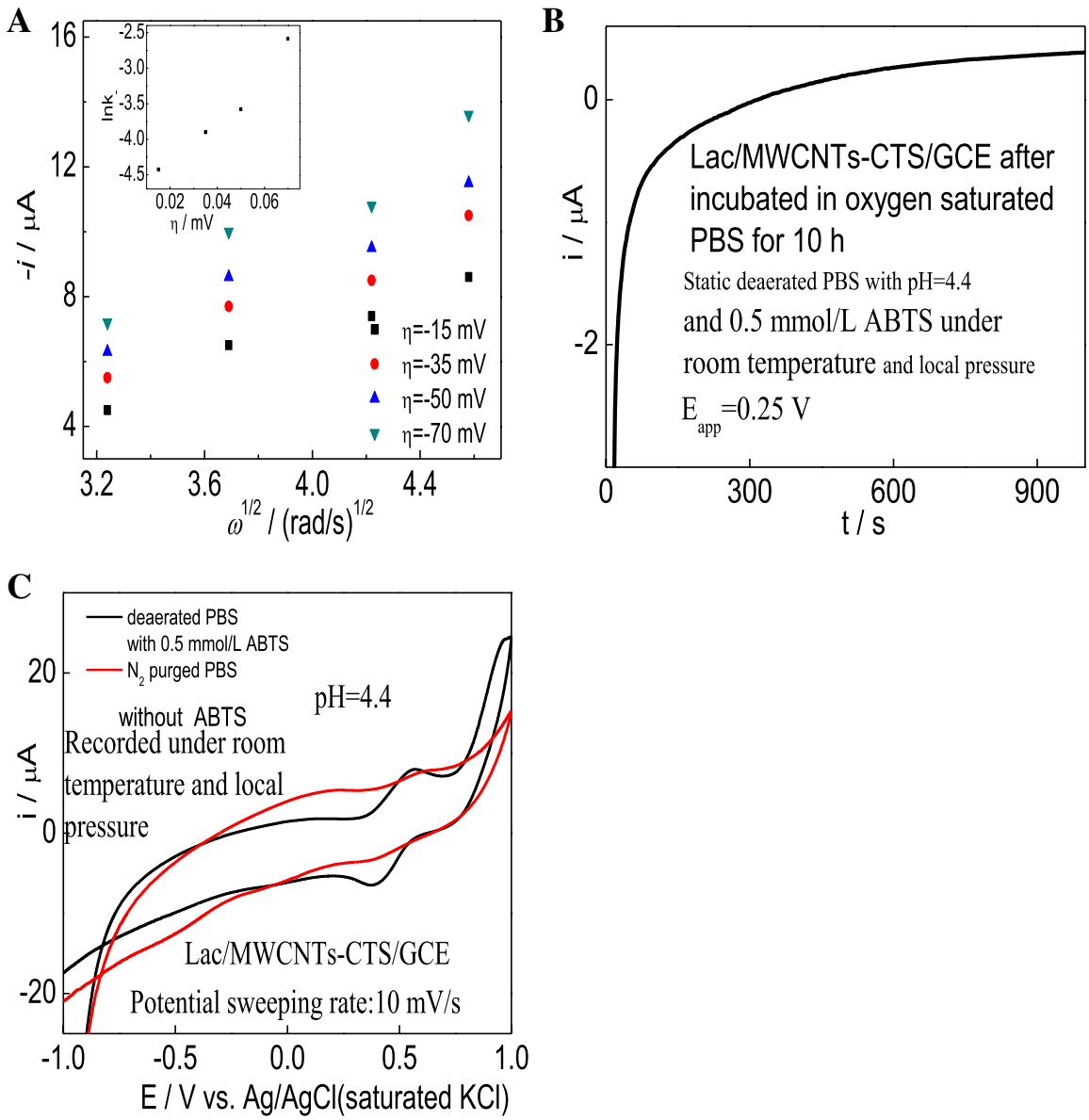

Fig. 7 Relationship *curves* of recorded current within the hybrid controlled zone of mass transferring and kinetics vs. square root of angular velocity for disk electrode at different over-potentials (**a**) and its *inset graph* dependence plot of logarithm value for calculated rate constant in electro-reduction of oxidized ABTS on over-potential away from formal potential of ABTS; chronoamperometric curve of electrode over-coated by nano-composite with Lac which was immersed in oxygen purged PBS for 10 h under applied potential of 0.25 V, data were recorded in N_2 saturated PBS with 0.5 mM ABTS (**b**); cyclic voltammograms of nano-complex modified electrode with Lac in deaerated PBS with ABTS and Lac-based electrode which was incubated efficiently in deaerated PBS with ABTS initially and then immersed in nitrogen purged PBS in the absence of ABTS (**c**)

result was in consistent with the conclusion which was drawn from the determination in oxygen content conducted withClark electrode. Analysis in Fig. 7c also exhibited that no apparent redox signal for nano-complex modified electrode with Lac which was incubated in deaerated PBS containing ABTS for 10 h and then transferred into the N_2 bubbled electrolyte without ABTS, was observed within the same sweeping range of potential).

3.1.5 Confirmation of Rate Limiting Step for Mediated ORR Induced by Incorporated Lac

Diffusion of dissolved mediator could be attributed to the rate limiting step in the whole mediated ORR of Lac-based electrode after comparison in normalized rate constants of each step under the same dimension (i.e. this value was only at the level of 10^{-4} s). This conclusion can also be applied to other systems in references. Similar results to Fig. 7b, c were

observed through repetition of tests to systems of Table 1. All these results indicated that the premise which had been discussed previously could be met according to the same method in this article. Table 1 illustrated rate constants of steps involved in mediated oxygen reduction under the same dimension for different Lac based electrodes. It was apparent that mass transferring of mediator should be the key factor in restraining the performance of enzymatic catalysis. The only valid way to improve the performance of this sub-case for mediated ORR induced by Lac integration in nano-complex was the replacement of electron relay with high efficiency. It meant that the preparation of electron mediator with higher apparent diffusion co-efficient and closer potential to formal one of redox protein molecules should be necessary. It also suggested small organic molecule which contained the structural unit of ferrocene with functionalized groups of azobenzene or other hetero-aromatic cycle may be a promising candidate.

3.2 External Influence on Lac Induced Catalysis to ORR

Figure 8 depicted the relationship between catalytic function on ORR and pH or testing temperature of electrolyte for nano-composite based electrode with Lac in aid of ABTS as electron mediator. It can be deduced from Fig. 8 that the bell shape reflecting the dependence of catalytic efficiency in Lac induced ORR on pH of PBS for Lac-based electrode was similar to that which has been described previously [30]. Difference in optimal pH between them was attributed to the influence of chemical composition and microenvironment of enzyme carrier on catalytic effect of ORR. Conclusion was also drawn from Fig. 8 the relationship between catalytic performance in ORR and temperature of PBS was similar to that which has been depicted elsewhere [30]. On the basis of the fact which was presented in Sect. 3.1.1, incorporation of Lac into nano-composite for the system in this article should be classified into a typical case of physical adsorption. It should be noted that difference in optimal temperature of catalysis for both systems could be ascribed to variable interactions between enzyme and matrix resulting from distinct

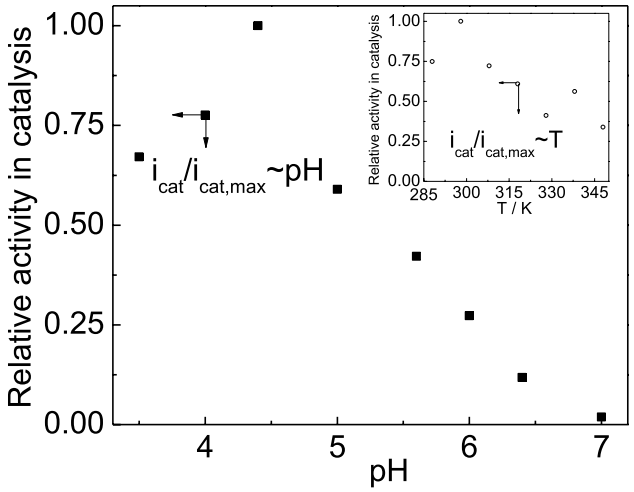

Fig. 8 Dependence of performance in catalysis to mediated ORR on pH and operating temperature of PBS saturated with oxygen in the presence of ABTS (0.5 mM) for Lac/MWCNTs-CTS/GCE recorded at scanning rate of 5 mV/s

conductive supports. It should be identified the influence of temperature on the performance of mediated ORR for Lac-based electrode in the presence of free electron mediator is self-contradictory: one hand the elevation in temperature enhances the dynamics in mass transferring of substrate and electron relay; on another hand over-oxidation of electron relay or complicated interaction between mediator and protein would deteriorate with the increasing of temperature and the catalytic effect of enzyme or capability of electron transferring of relay would degenerate consequently (This complex impact on catalytic efficiency of ambient temperature could be observed in Fig. 8).

4 Conclusion

Kinetics of mediated ORR for nano-composite based electrode with incorporated Lac was probed with spectroscopy and electrochemistry. Rate constants of steps involved in the catalytic cycle were compared under the same dimension.

Table 1 Kinetics analysis in each step involved in catalytic cycle for Lac-based electrodes under the same dimension: s^{-1}

Lac-based electrode	Rate of mediator diffusion		Rate for Lac induced oxidation of mediator	Rate for Lac-induced binding of O_2	Electrochemical reaction rate of mediator
	Oxidized	Reduced			
Lac based electrode, mediator: ABTS [13]	6.3×10^{-5}	6.0×10^{-5}	1.43	430.2	0.07
Lac based electrode, mediator: ABTS [26]	7.5×10^{-5}	6.8×10^{-5}	0.16	770.3	0.005
Lac based electrode, mediator: 1,1′-ferrocenedimethanol [29]	2.7×10^{-5}	2.1×10^{-5}	2.88	158.2	0.02

Diffusion coefficient of substrate in the aqueous solution was almost the same in the absence of selective adsorption of oxygen molecules on the matrix

Those steps included mass transferring of substrate and mediator under oxidized and reduced state, Lac-involved chemical reactions which consisted of oxidation of mediator, substrate transformation and oxygen attachment on active site of enzyme as well as electro-reduction of oxidized ABTS. Thus rate limiting step was ascribed to the process of mediator diffusion only when the precondition that the accommodation amount of mediator and substrate within the matrix can be regarded to be fiddling could be met. It should be noted the composition of enzyme carrier and the interaction between matrix and incorporated protein would pose influence on many aspects of Lac-based electrode such as morphology and electric conductivity of nano-composite with enzyme, mechanical stability of thin film made up of nano-complex with incorporated enzyme, performance in electron transferring between active sites in Lac and conductive support, thermal stability and acid-base tolerance in catalytic performance ofORR for Lac-based electrode.

Acknowledgements The study was financially supported by the National Natural Science Foundation of China (No. 21363024) and Science and Technology Innovation Funding Project of Graduate Students in Xinjiang Normal University (XSY201502009).

References

1. Y.J. Zhang, M. Chu, L. Yang, Y.M. Tan, W.F. Deng, M. Ma, X.L. Su, Q.J. Xie, ACS Appl. Mater. Interfaces **6**, 12808 (2014)
2. M.S. Kilic, S. Korkut, B. Hazer, E. Erhan, Biosens. Bioelectron. **61**, 500 (2014)
3. M. Falk, Z. Blum, S. Shleev, Electrochim. Acta **82**, 191 (2012)
4. K.P. Lee, A.I. Gopalan, S. Komathi, Sens. Actuators B **141**, 518 (2009)
5. T. Kuwahara, K. Nakata, M. Kondo, M. Shimomura, Synth. Met. **214**, 30 (2016)
6. W.S. Huo, H. Zeng, Y. Yang, Y.H. Zhang, Chem. Phys. Lett. **671**, 15 (2017)
7. M. Zhou, L. Deng, D. Wen, L. Shang, L.H. Jin, S.J. Dong, Biosens. Bioelectron. **24**, 2904 (2009)
8. A. Ressine, C. Vaz-Dominguez, V.M. Fernandez, A.L. De Lacey, T. Laurell, T. Ruzgas, S. Shleev, Biosens. Bioelectron. **25**, 1001 (2010)
9. S. Tsujimura, H. Tatsumi, J. Ogawa, S. Shimizu, K. Kano, T. Ikeda, J. Electroanal. Chem. **496**, 69 (2001)
10. G.T.R. Palmore, H.H. Kim, J. Electroanal. Chem. **464**, 110 (1999)
11. Y.M. Yan, W. Zheng, L. Su, L.Q. Mao, Adv. Mater. **18**, 2639 (2006)
12. Y.Y. Zhang, M.A. Arugula, S.T. Williams, S.D. Minteer, A.L. Simonian, J. Electrochem. Soc. **163**, F449 (2016)
13. W. Zheng, J.Y. Ma, F. Guo, J. Li, H.M. Zhou, X.X. Xu, L. Li, Y.F. Zheng, Bio Med. Mater. Eng. **24**, 229 (2014)
14. K. Karnicka, K. Miecznikowski, B. Kowalewska, M. Skunik, M. Opallo, J. Rogalski, W. Schuhmann, P.J. Kulesza, Anal. Chem. **80**, 7643 (2008)
15. J.F. Fei, H.K. Song, G.T.R. Palmore, Chem. Mater. **19**, 1565 (2007)
16. W.E. Farneth, B.A. Diner, T.D. Gierke, M.B. D'Amore, J. Electroanal. Chem. **581**, 190 (2005)
17. Y. Ogino, K. Takagi, K. Kano, T. Ikeda, J. Electroanal. Chem. **396**, 517 (1995)
18. W.E. Farneth, M.B. D'Amore, J. Electroanal. Chem. **581**, 197 (2005)
19. N.S. Parimi, Y. Umasankar, P. Atanassov, R.P. Ramasamy, ACS Catal **2**, 38 (2012)
20. Y. Liu, X.H. Qu, H.W. Guo, H.J. Chen, B.F. Liu, S.J. Dong, Biosens. Bioelectron. **21**, 2195 (2006)
21. W. Zheng, H.M. Zhou, Y.F. Zheng, N. Wang, Chem. Phys. Lett. **457**, 381 (2008)
22. S. Tsujimura, Y. Kamitaka, K. Kano, Fuel Cells **7**, 463 (2007)
23. H. Zeng, Z.Q. Tang, L.W. Liao, J. Kang, Y.X. Chen, Chin. J. Chem. Phys. **24**, 653 (2011)
24. J. Huang, J.Y. Zhou, H.Y. Xiao, S.Y. Long, J.T. Wang, Acta. Chim. Sin. **63**, 1343 (2005). (**In Chinese**)
25. H.J. Qiu, C.X. Xu, X.R. Huang, Y. Ding, Y.B. Qu, P.J. Gao, J. Phys. Chem. C **113**, 2521 (2009)
26. W. Wei, P.P. Li, Y. Li, X.D. Cao, S.Q. Liu, Electrochem. Commun. **22**, 181 (2012)
27. H.Y. Zhao, H.M. Zhou, J.X. Zhang, W. Zheng, Y.F. Zheng, Biosens. Bioelectron. **25**, 463 (2009)
28. Y.F. Zhu, S. Kaskel, J.L. Shi, T. Wage, K-H.V. Pee, Chem. Mater. **19**, 6408 (2007)
29. M. Klis, M. Karbarz, Z. Stojek, J. Rogalski, R. Bilewicz, J. Phys. Chem. B **113**, 6062 (2009)
30. D.S. Jiang, S.Y. Long, J. Huang, H.Y. Xiao, J.Y. Zhou, Biochem. Eng. J **25**, 15 (2005)